Identification of unusual butanetriol dialkyl glycerol tetraether and pentanetriol dialkyl glycerol tetraether lipids in marine sediments

Chun Zhu*, Travis B. Meador, Wolf Dummann, Kai-Uwe Hinrichs

MARUM Center for Marine Environmental Sciences and Department of Geosciences, University of Bremen, 28334 Bremen, Germany

*corresponding author; czhu@uni-bremen.de

Running head: Butanetriol or pentanetriol-based tetraether lipids

Abstract

RATIONALE: Glycerol serves as the principal backbone moiety bound to various acyl/alkyl chains for membrane lipids of *Eukarya*, *Bacteria*, and *Archaea*. In this study, we report a suite of unusual tetraether lipids in which one of the two conventional glycerol backbones is substituted by butanetriol or pentanetriol.

METHODS: Identification of these lipids was achieved via diagnostic fragments and their expected acetylation products using liquid chromatography-mass spectrometry (LC-MS), and their diagnostic ether cleavage products using gas chromatograph-mass spectrometry (GC-MS).

RESULTS: We observed structural variations in the polyol backbones and alkyl chains and term these core lipid derivatives: isoprenoidal butanetriol dialkyl glycerol tetraethers (iso-BDGTs), isoprenoidal pentanetriol dialkyl glycerol tetraethers (iso-PDGTs), and hybrid isoprenoidal/branched BDGTs and PDGTs (ib-BDGTs, ib-PDGTs). Of these, iso-BDGTs were the most abundant with a methylation at either *sn*-1 or *sn*-3 position of glycerol and were also found as part of intact polar lipids, adjoined to mono- or diglycosidic headgroups. Iso-BDGTs and iso-PDGTs are likely produced by *Archaea*, as indicated by the presence of the characteristic biphytanyl moieties.

CONCLUSIONS: Butanetriol and pentanetriol-based tetraether lipids occur in modern estuarine and deeply buried subseafloor sediments, suggesting the presence of alternative backbones in archaeal lipids.

Key words: glycerol, butanetriol, pentanetriol, tetraether lipids, lipid backbone

1. Introduction

Glycerol serves as a backbone moiety bound to acyl/alkyl chains and polar head groups, forming the major membrane lipids found in nature. Archaeal lipids primarily comprise isoprenoidal dialkyl glycerol diethers (iso-DGDs) and isoprenoidal glycerol dialkyl glycerol tetraethers (iso-GDGTs). The glycerol backbone of archaeal lipids is derived from *sn*-glycerol-1-phosphate (G1P; Kates, 1978), the enantiomer of *sn*-glycerol-3-phosphate (G3P) used to form the backbone of bacterial and eukaryotic membrane lipids. The stereochemistry of the glycerol backbone represents a chemotaxonomic hallmark that distinguishes *Archaea* from the other two life domains (Kates, 1978).

Biosynthesis of glycerol ether lipids in archaea involves dihydroxyacetonephosphate (DHAP), which is subsequently reduced by *sn*-glycerol-1-phosphate dehydrogenase (G1PDH) to form G1P (Koga and Morii, 2007; Pereto et al., 2004). However, the detection of tetritoldiphytanyl diether (TDD; de Rosa et al., 1986), in which a tetritol replaces the glycerol backbone bound to two isoprenoidal alkyl chains, implies an alternative initial substrate for archaeal ether lipid biosynthesis. Nevertheless, TDD was only reported in *Methanosarcina barkeri* and *Methanosarcina mazei* as a minor archaeal lipid (de Rosa and Gambacorta, 1988; de Rosa et al., 1986), such that one might view TDD as a metabolic byproduct during lipid biosynthesis. Recently, Knappy (2013) reported unusual tetraether lipids bearing one or two extra carbons relative to the archaeal GDGTs; these were tentatively assigned as homoglycerol tetraether lipids with an additional saturated C-C bond(s). However, the position of the additional C-C bond remains unknown.

Here, we provide three lines of evidence to confirm the existence of unusual tetraether lipids with 1,2,3-butanetriol as one of the two termini bound to dibiphytanyl alkyl chains, which we

termed isoprenoidal butanetriol dialkyl glycerol tetraethers (iso-BDGTs). Moreover, several ions exhibited similar retention time and fragmentation patterns after liquid chromatography-tandem mass spectrometry (LC-MS^2), revealing a series of iso-BDGT homologues, which we tentatively assigned as isoprenoidal pentanetriol dialkyl glycerol tetraethers (iso-PDGTs) as well as their corresponding glycolipids and hybrid isoprenoidal/branched (cf. Liu et al., 2012) BDGTs and PDGTs (ib-BDGTs and ib-PDGTs). These unusual ether lipids are detected in shallow estuarine and deeply buried subsurface deep-sea sediments, indicating the existence of a butanetriol/pentanetriol-based lipid biosynthesis pathway.

2. Experimental

2.1. Materials

A shallow estuarine sediment sample was collected from the White Oak River Estuary (WORE, Lloyd et al., 2009), North Carolina, USA, in October 2010; a deep subsurface sediment sample with approximate age of 1 Ma was obtained from the Peru Margin during Ocean Drilling Program Leg 201 (D'Hondt et al., 2003). This initial sample set spans geographically and temporally distinct sediment regimes. Standards of glycerol, 1,2,3-butanetriol, and 1,2,4-butanetriol were purchased from Sigma-Aldrich GmbH, Munich, Germany.

2.2. Sample preparation

The sample preparation procedure is summarized in Scheme 1. Total lipid extracts (TLEs) were obtained from freeze-dried and homogenized sediments using a modified Bligh and Dyer protocol (Sturt et al., 2004). TLEs were separated into fractions of core lipids (CLs, without head groups) and intact polar lipids (IPLs, with head groups) after preparative chromatography, using

an Intersil Diol column (150 × 10 mm, 5 µm particle size; GL Sciences Inc., Tokyo, Japan) installed in an Agilent 1200 series HPLC equipped with an Agilent 1200 series fraction collector. TLEs were dissolved in *n*-hexane:2-propanol (7:3, v/v) prior to injection and were eluted using a binary solvent system consisting of *n*-hexane: 2-propanol (85:15, v/v; eluent A) and 2-propanol: water (90:10, v/v; eluent B). The gradient ramped from 0% B to 10% B at 5 min, and then to 100% B at 6 min, subsequently holding for 10 min; the flow rate was 3 mL min^{-1}. The column was maintained at 30°C and re-equilibrated with 100% A for 10 min before the next injection. CL and IPL fractions were collected in the time windows of 1.0-5.1 min and 5.1-12 min, respectively. Carryover of CLs into the IPL fraction was minor (typically <1%) as determined by liquid chromatography-mass spectrometry (LC-MS). Aliquots of the IPL fractions were hydrolyzed in a mixture of 6M HCl/methanol/dichloromethane (1:9:1, v/v) at 70°C for 24 h (Lipp and Hinrichs, 2009), which converts IPLs to CLs by cleaving the polar head groups.

Target iso-BDGTs and iso-GDGTs were further isolated from the CL fraction after preparative HPLC using a PerfectSil 100 CN-3 column (250 × 10 mm, 5 µm particle size, MZ Analysentechnik, Germany). CL mixtures were dissolved in *n*-hexane/2-propanol (99:1, v/v) and eluted isocratically with 100% A for 1 min, followed by a slow gradient to 10% B over 14 min, and then increased to 60% B over another 15 min at a flow rate of 3 mL/min. Eluent A was *n*-hexane/2-propanol (99:1, v/v) and B was *n*-hexane/2-propanol (90:10, v/v). The column temperature was 25°C. The column was washed for 15 min with 100% B and then another 15 min with 100% A before each injection. Iso-BDGTs and iso-GDGTs were collected in the time intervals of 11.0-13.0 min and 13.1-18.0 min, respectively. Purity was monitored by LC-MS, which confirmed that iso-BDGTs dominated the iso-BDGT fraction and were not detected in the iso-GDGT fraction. An aliquot of each fraction was then subjected to ether cleavage (after Lin et

al., 2012) to obtain tetraether-derived triols and biphytanes. Alcohols were derivatized by N,O-bis(trimethylsilyl)trifluoroacetamide (BSTFA) prior to gas chromatography-mass spectrometry (GC-MS) analysis (Lin et al., 2012).

Aliquots of the CL fraction were acetylated by adding 100 µL acetic anhydride (Sigma-Aldrich, Steinheim, Germany) and 20 µL 1-methylimidalzole (Sigma-Aldrich, Steinheim, Germany) to the dry sample. The headspace was replaced with N_2 before tightening caps and the reaction vials were kept at room temperature for 15 min, after which excess acetic anhydride was quenched by adding 0.5 mL water. After 10 min, 0.5 mL methylene chloride was added to extract the acetylated CLs. This was repeated 3 times and the extracts were combined and dried under N_2. Samples were then resuspended in 0.5 mL hexane and dried under N_2; this was repeated 3 times before samples were finally suspended in the injection solvent and analyzed by LC-MS as above.

2.3. Instrumental analysis

CL analysis was performed using a Dionex Ultimate 3000 ultra-high pressure LC (UHPLC) coupled to a Bruker maXis Ultra-High Resolution quadrupole time-of-flight mass spectrometer (qTOF-MS) via an APCI II ion source according to Becker et al. (2013). IPLs were analyzed with the same qTOF-MS instrument using the method by Zhu et al. (2013). MS^2 spectra for both CL and IPL analysis were recorded using automated data-dependent fragmentation of the three most abundant ions that were selected for collision induced dissociation (CID). Acetylated CLs were analyzed according to Liu et al. (2012), using an Agilent 6130 MSD single quadrupole mass spectrometer coupled to an Agilent 1200 series HPLC via an APCI ion source. GC-MS analyses of tetraether lipid-derived triols and biphytanes were performed on an Agilent 5973

125 inert MSD system equipped with a Restek Rxi-5ms column (30 m × 250 µm × 0.25 µm, Restek,
126 Bad Homburg, Germany) as described by Lin et al. (2012).
127
128 **3. Results and discussion**
129 *3.1. LC-MS identification*
130 LC-MS^2 analysis of modern and ancient sediments revealed iso-GDGT lipids containing 0-4
131 cyclopentyl and up to one cyclohexyl moiety in the isoprenoidal chains (*m/z* 1302.3 - 1292.3).
132 Notably, we observed three isobaric ions of *m/z* 1316.3401, 1316.3398, and 1316.3381 (Fig. 1A;
133 peaks **I**,**III**, and **IV,** respectively) and one of *m/z* 1330.3356 (Fig. 1A; peak **II**), whose protonated
134 formulae correspond to $[C_{87}H_{175}O_6]^+$ (<1 ppm) for peaks **I**, **III**, **IV** and $[C_{88}H_{177}O_6]^+$ (<1 ppm)
135 for **II**, indicating the presence of one or two additional methylene moieties compared to the
136 acyclic iso-GDGT (*m/z* 1302.3), respectively. Methoxy acyclic iso-GDGT (Knappy et al., 2009)
137 and methylated acyclic iso-GDGT, which has a methyl group substitution at the C-13 position
138 (i.e., homocaldarchaeol; Galliker et al., 1998), have been previously reported and share the same
139 protonated chemical formulae as peaks **I**, **III**, and **IV**. These compounds can be identified by the
140 differences in their polarities and MS^2 spectra (e.g., Knappy et al., 2009). After fragmentation,
141 peak **I** displayed product ions of *m/z* 1284.3 and 757.7, consistent with neutral losses of methanol
142 (32.0 Da) and one of the two constituent biphytanyl chains (557.6 Da), respectively. The *m/z*
143 743.7 ion was absent (Fig. 1D), indicating that the additional methyl group was etherified at one
144 of two terminal hydroxyl groups of acyclic iso-GDGT (Knappy et al., 2009). In contrast,
145 fragmentation of peak **IV** (Fig. 1E) is characterized by product ions of *m/z* 743.7 and 1242.3,
146 derived from cleavage of a methylated biphytadiene and a $C_3H_6O_2$ unit, respectively, indicating

147 incorporation of the additional methyl group into one of the two alkyl chains. Therefore, peaks **I**
148 and **IV** are assigned as acyclic methoxy acyclic iso-GDGT and homocaldarchaeol, respectively.

149 The MS^2 spectrum of peak **III** (*m/z* 1316.3398) displays two clusters of product ions (Fig.
150 1B). The higher mass products result from losses of water and other small molecules from the
151 precursor ions and the lower mass products are formed after dissociation of one alkyl chain
152 ($C_{40}H_{80}$, *m/z* 557.6) and concomitant/sequential elimination of 1-4 molecules of water and other
153 small molecules during CID (Fig. 1B), consistent with the typical fragmentation of archaeal
154 GDGTs (Knappy et al., 2009; Liu et al., 2012; Becker et al., 2013). However, there are subtle,
155 informative differences. After CID, peak **III** generates a strong product ion of *m/z* 1228.3,
156 derived from a loss of $C_4H_8O_2$ (88.1 Da), rather than the typical $C_3H_6O_2$ (74.0 Da) of
157 conventional GDGTs. Furthermore, the product ion of *m/z* 1284.3 that is generated from
158 methoxy acyclic iso-GDGT (*m/z* 1316.3401) via cleavage of a terminal methanol (cf. Fig. 1D) is
159 absent. Such fragments likely indicate that the additional carbon atom bound directly to the triol
160 backbone moiety but not as a methoxy group. This is evidence for the possible presence of a
161 butanetriol rather than methoxy glycerol as one terminus for peak **III**. Likewise, the MS^2
162 spectrum of peak **II** (*m/z* 1330.3356) shows a strong ion of *m/z* 1228.3 formed by the neutral loss
163 of $C_5H_{10}O_2$ (102.1 Da), indicating the presence of a pentanetriol terminus (Fig. 1B). Consistent
164 with this interpretation, the polarities of peaks **II** and **III** are intermediate, eluting between the
165 relatively more apolar methoxy acyclic iso-GDGT (**I**) and more polar homocaldarchaeol (**IV**)
166 after normal phase chromatography (Fig. 1A).

167 After an acetylation reaction, only the di-acetylated product of peak **III** (*m/z* 1400.2) was
168 detected (data not shown), further confirming that the additional methyl group located within the
169 backbone-triol moiety was part of a C_4 carbon chain rather than a methoxy derivative; the latter

molecule would have received only one acetyl group on the opposite glycerol terminus. Parallel analysis of an acyclic iso-GDGT standard (*m/z* 1302.3) indicated a high yield of the di-acetylated product (i.e., *m/z* 1386.3) while the *m/z* 1302.3 ion and the mono-acetylated product were not detectable after acetylation. We thus assign peak **III** as isoprenoidal acyclic butanetriol dialkyl glycerol tetraether (iso-$BDGT_0$) and, by inference, peak **II** as isoprenoidal acyclic pentanetriol dialkyl glycerol tetraether (iso-$PDGT_0$). We note that iso-$PDGT_0$ was below the detection limit in the TLE from the White Oak River Estuary analyzed for the acetylation experiment.

3.2. GC-MS identification

The proposed butanetriol backbone of compound **III** may have constitutional isomers such as 1,2,3-butanetriol and 1,2,4-butanetriol, and the $C_{40}H_{80}$ alkyl moieties may also have isomers alternative to the typical biphytanyl chains. Both the alternative backbones and the associated alkyl moieties cannot be confirmed by LC-MS^2 alone. We thus analyzed the alcohol and hydrocarbon products after ether cleavage of a concentrated BDGT fraction by GC-MS. As expected, glycerol (detected as a TMS derivative) and biphytanes with 0-2 cyclopentyl moieties were detected, consistent with the products observed for GDGTs (suppl. Figure). An additional product, identified as 1,2,3-butanetriol, was only present in the BDGT fraction but not in the GDGT fraction (Fig. 2), corroborating the structural assignment based on the LC-MS^2 and the acetylation experiments. We thus conclude that the backbone corresponds to a glycerol methylated at either the *sn*-1 or *sn*-3 position to form the 1,2,3-butanetriol backbone (Fig. 3). These compounds differ from 1,2,4-butanetriol backbone-based lipids found in some eukaryotes (Vaver et al., 1964; 1967). Although the exact stereochemistry of the butanetriol backbone remains to be determined, the iso-BDGTs containing isoprenoidal tetraether moieties are

structurally related analogues of archaeal iso-GDGTs, strongly suggesting that they are biosynthetic products of certain members of *Archaea*. We did not detect pentanetriol as an ether cleavage product, likely due to poor recovery combined with the low concentration of iso-PDGTs in the sample from White Oak River Estuary used for this experiment. However, as homologues of iso-BDGTs, an archaeal origin of iso-PDGTs is suggested.

3.3. IPL counterparts and analogues

Iso-BDGTs bearing 0-3 cyclopentanyl rings (iso-$BDGT_{0-3}$) and their IPL counterparts, present as mono- and di-glycosidic iso-BDGTs (1G-, 2G-iso-BDGTs; Fig. 3), were also detected in estuarine sediments with LC-MS^2 (Fig. 1F and G). These head groups are common in archaeal IPLs found in marine sediments and were assigned according to diagnostic neutral losses (e.g., Sturt et al., 2004). Analysis of acid hydrolysis products of IPLs confirmed the core structures as iso-BDGTs rather than homocaldarchaeol and revealed that IPL-iso-BDGTs accounted for significant proportions (~10% and ~30% for subseafloor Peru margin and modern estuarine sediments, respectively, based on the relative MS responses) of total archaeal IPLs.

Based on differences in the alkyl chains, Liu et al. (2012) broadly designated GDGT lipids into five groups, including isoprenoidal GDGTs (iso-GDGTs; C_{86}), hybrid isoprenoidal/branched GDGTs (ib-GDGTs; $C_{74\text{-}80}$), overly branched GDGTs (ob-GDGTs; $C_{69\text{-}74}$), conventional branched GDGTs (b-GDGTs; $C_{66\text{-}68}$), and sparsely branched GDGTs (sb-GDGTs; $C_{62\text{-}65}$). We observed BDGTs and PDGTs bearing hybrid isoprenoidal/branched alkyl moieties, termed ib-BDGTs ($C_{76\text{-}81}$) and ib-PDGTs ($C_{77\text{-}82}$). These compounds were identified based on their retention pattern as well as diagnostic neutral losses of $C_4H_8O_2$ (88.1 Da) and $C_5H_{10}O_2$ (102.1 Da), respectively (Fig. 3 and 4). However, BDGTs or PDGTs with other alkyl moieties (i.e., b-,

ob-, or sb-GDGTs) were not detected, possibly due to their low concentrations or the lack of biosynthetic pathways producing these lipids.

3.4. Implications

There are multiple proposed pathways of archaeal polar lipid biosynthesis, however dihydroxyacetone phosphate (DHAP) has been accepted as an initial substrate (Koga and Morii, 2007; Nishihara et al., 1999). The spatially and temporally widespread BDGT and PDGT lipids likely indicate the use of alternative substrates by *Archaea* during the initiation of lipid biosynthesis. The enzyme involved in DHAP reduction is stereo-specific, which leads to the formation of G1P (Kates, 1978). Enzymes catalyzing the formation of $C_{4\text{-}5}$ polyol backbone for iso-BDGTs and iso-PDGTs may also be stereo-specific. Because the detected 1,2,3-butanetriol lipid backbone has two stereogenic centers, any of the possible four isomers (enantiomers and diastereoisomers) could serve as a novel backbone for these lipids. The occurrence of BDGT and PDGT lipids in environmental samples, as well as tetritoldiphytanyl diether lipids in archaeal cultures (de Rosa et al., 1986), suggests that in addition to glycerol and calditol, archaea are able to use 1,2,3-butanetriol, pentanetriol, and tetritol as backbones for their membrane lipids. Because chemotaxonomic and functional diversity of membrane lipids is largely reflected by lipid structural variation (Fahy et al., 2011), future studies should determine the properties of butanetriol and pentanetriol-based ether lipids, including their stereochemistry, biological functions, and biosynthetic pathways.

Conclusions

We report a suite of unusual tetraether lipids, characterized by the replacement of one terminal glycerol moiety with a butanetriol or pentanetriol that is bound to either isoprenoidal or hybrid isoprenoidal/branched alkyl chains. We term these lipids as iso-BDGTs, iso-PDGTs, ib-BDGTs, and ib-PDGTs. IPL-iso-BDGTs (i.e., 1G- and 2G-iso-BDGTs) were also detected and accounted for significant proportions of total sedimentary archaeal IPLs in our studied samples. Although the stereochemistry of such $C_{4\text{-}5}$ backbones remains to be determined, the iso-BDGTs and iso-PDGTs are structurally related analogues of archaeal iso-GDGTs, consistent with an archaeal source, whereas the sources of ib-BDGTs and ib-PDGTs remain unknown. These butanetriol and pentanetriol-based tetraether lipids were detected in estuarine and deep-sea subseafloor sediments, suggesting polyol backbone diversity in tetraether lipids and the flexibility of prokaryotes to utilize additional substrates during membrane lipid biosynthesis.

Acknowledgements

This work was funded by the Deutsche Forschungsgemeinschaft (DFG) by a postdoctoral fellowship granted through the Cluster of Excellence/Research Center MARUM to C.Z., and funded by the European Research Council under the European Union's Seventh Framework Programme–"Ideas" Specific Programme, ERC grant agreement No. 247153 (K.-U.H.). Sherif Ghobrial and Cassandre Lazar are acknowledged for their participation in the collections of estuarine sediment samples from the White Oak River Estuary. We acknowledge the ODP Leg 201 Shipboard Scientific Party for sample collection, and we also thank two anonymous reviewers for constructive comments.

References

Becker, K.W., Lipp, J.S., Zhu, C., Liu, X. and Hinrichs, K.-U. An improved method for the analysis of archaeal and bacterial ether core lipids. *Org. Geochem.* **2013**, *61*, 34-44.

D'Hondt, S.L., Jørgensen, B.B., Miller, D.J., Shipboard Scientific Party. Proceedings of the Ocean Drilling Program, initial reports. (ocean drilling program, Texas A &M University, College Station, TX) **2003**, 201. doi:10.2973/odp.proc.ir.201.2003.

De Rosa M., Gambacorta A. The lipids of archaebacteria. *Prog. Lipid Res.* **1988**, 27, 153-175.

De Rosa M., Gambacorta A., Lanzotti V., Trincone A., Harris J.E., Grant W.D. A range of ether core lipids from the methanogenic archaebacterium *Methanosarcina-barkeri*. *Biochim. et Biophys. Acta* **1986**, 875, 487-492.

Fahy E., Cotter D., Sud M., Subramaniam S. Lipid classification, structures and tools. *Biochim. Biophys. Acta* **2011**, 1811, 637-647.

Galliker, P., Gräther, O., Rümmler, M., Fitz, W., Arigoni, D. New structural and biosynthetic aspects of the unusual core lipids from *Archaebacteria*. In Vitamin B_{12} and B_{12}-proteins, Krautler, B., Arigoni, D., Golding, B. T., Eds.; Wiley-VCH: Hoboken **1998**, 447– 458.

Kates, M. The phytanyl ether-linked polar lipids and isoprenoid neutral lipids of extremely halophilic bacteria. *Prog. Chem. Fats Other Lipids* **1978**, 15, 301–342.

Knappy C. S. Mass spectrometric studies of ether lipids in Archaea and sediments, *PhD thesis*, 2010 (publication in April **2013** after embargo was lifted), University of York.

Knappy C.S., Chong J.P.J., Keely B.J. Rapid discrimination of archaeal tetraether lipid cores by liquid chromatography-tandem mass spectrometry. *J. Am. Soc. Mass Spectrom.* **2009**, 20, 51-59.

Koga Y., Morii H. Biosynthesis of ether-type polar lipids in archaea and evolutionary considerations. *Microbiol. Mol. Biol. Rev.* **2007**, 71, 97-120.

284 Lin Y-S, Lipp J. S., Elvert M., Holler T., and K-U Hinrichs. Assessing production of the
285 ubiquitous archaeal diglycosyl tetraether lipids in marine subsurface sediment using
286 intramolecular stable isotope probing. *Environ. Microbiol.* **2012**, 15, 1634-1646
287 Lipp J.S. and Hinrichs K.U. Structural diversity and fate of intact polar lipids in marine
288 sediments. *Geochim. Cosmochim. Acta* **2009**, 73, A771-A771.
289 Liu X.L., Summons R.E., Hinrichs K.U. Extending the known range of glycerol ether lipids in
290 the environment: structural assignments based on tandem mass spectral fragmentation
291 patterns. *Rapid Commun. in Mass Spectrom.* **2012**, 26, 2295-2302.
292 Lloyd K. G., Alperin M. J. and Teske A. Environmental evidence for net methane production
293 and oxidation in putative ANaerobic MEthanotrophic (ANME) archaea. *Environ. Microbiol.*
294 **2009**, 13, 2548–2564
295 Nishihara M., Yamazaki T., Oshima T., Koga Y. Sn-Glycerol-1-phosphate-forming activities in
296 Archaea: Separation of archaeal phospholipid biosynthesis and glycerol catabolism by
297 glycerophosphate enantiomers. *J. of Bacteriol.* **1999**, 181, 1330-1333.
298 Pereto J., Lopez-Garcia P., Moreira D. Ancestral lipid biosynthesis and early membrane
299 evolution. *Trends in Biochem. Sci.* **2004**, 29, 469-477.
300 Sturt H.F., Summons R.E., Smith K., Elvert M., Hinrichs K.U. Intact polar membrane lipids in
301 prokaryotes and sediments deciphered by high-performance liquid
302 chromatography/electrospray ionization multistage mass spectrometry - new biomarkers for
303 biogeochemistry and microbial ecology. *Rapid Commun. in Mass Spectrom.* **2004**, 18, 617-
304 628.

Vaver, V.A, Ushakov A.N., and L.D. Bergelson. Identification and quantitative determination of diols and triols by the method of gas chromatography. *Izvestiya AkademiiNauk SSSR, Seriya Khimicheskaya*, **1967**, 392.

Vaver, V.A., Prokazova, N. V., and L.D. Bergelson. New types of neutral lipids. *Izvestiya AkademiiNauk SSSR, Seriya Khimicheskaya* **1964**. 6, 1187-1192.

Zhu, C., Lipp, J.S., Wörmer, L., Becjer, K.W., Schröder, J., Hinrichs, K.-U.. Comprehensive glycerol ether lipid fingerprints through a novel reverse-phase liquid chromatography-mass spectrometry protocol. *Org. Geochem.* **2013**, 42, 376-386.

Scheme

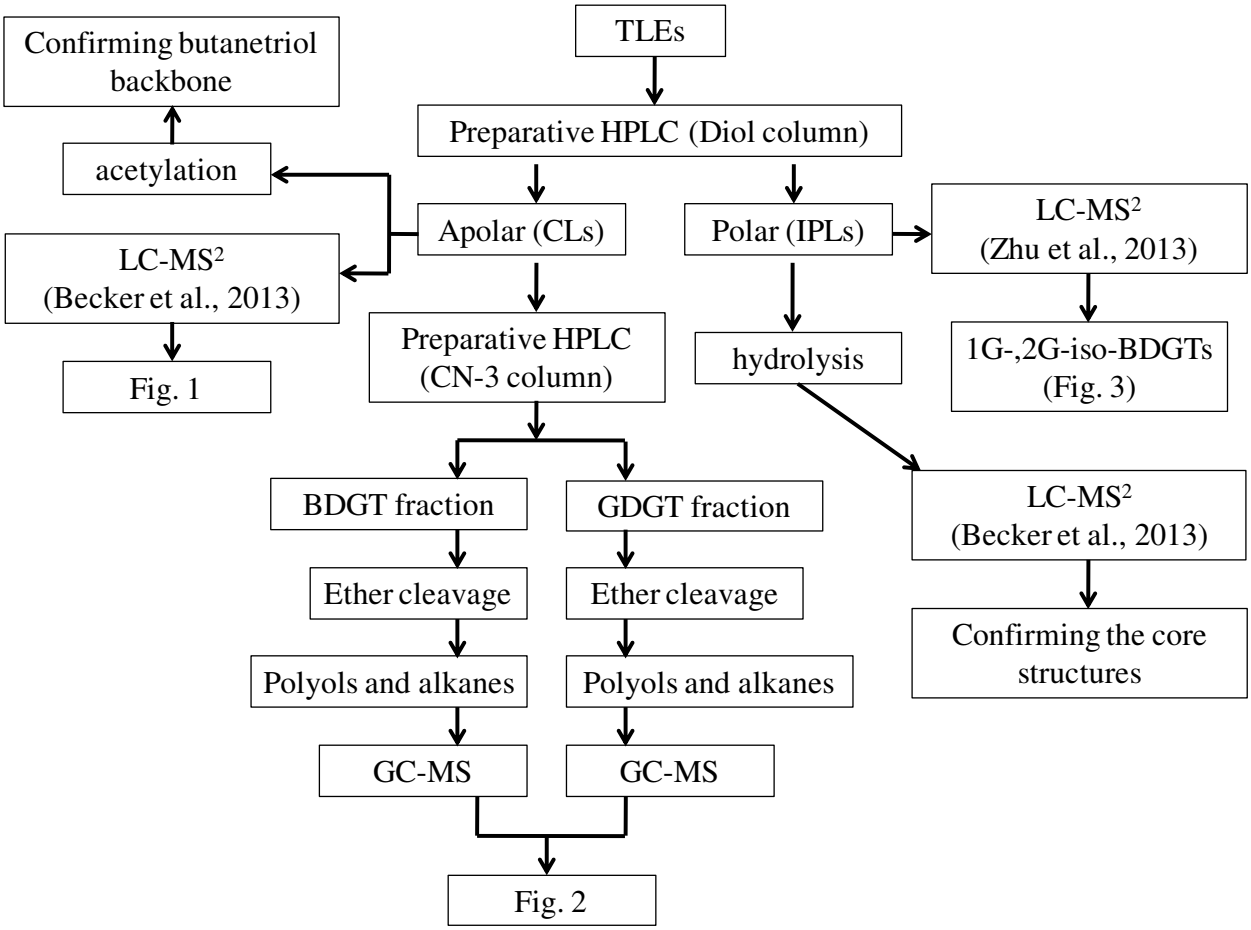

Scheme 1. Flowchart of the sample preparation procedure. CLs = core lipids, IPLs = intact polar lipids. The details of preparative HPLC are provided in the text.

Figure captions

Fig. 1. LC-MS^2 analysis of tetraether CLs (Panels A-E) in Peru margin sediments (Leg 201, 1229A-12H3, 102.75 meter below the seafloor) and IPLs (Panels F-G) in WORE sediments (0-20 cm). Panel A shows an extracted ion chromatogram (EIC) of protonated ions (peaks **I-IV**) that are 14.0 or 28.0 Da higher than protonated caldarchaeol (*m/z* 1302.3). Panels B-E show MS^2 spectra of **II** (B), **III** (C), **I** (D), **IV** (E), 1G-iso-$BDGT_0$ (F), and 2G-iso-$BDGT_0$ (G). Note, accurate masses (four digits) are used in panel A for constraint of the protonated lipid formulae, while masses with one digit are used in MS^2 spectra for simplicity, where protonated precursor ions are marked with blue diamonds (panels B-E). CL and IPL analysis was based on Becker et al. (2013) and Zhu et al, (2013), respectively.

Fig. 2. GC-MS analysis of TMS derivatives of 1,2,3-butanetriol standard and butanetriol products liberated from the ether cleavage of iso-BGDG and iso-GDGT fractions, which were purified from the total lipid extract of WORE sediments (0-20 cm).

Fig. 3. Constrained structures of iso-BDGTs, ib-BDGTs and ib-PDGTs detected in Peru Margin sediments (Leg 201, 1229A-12H3, 102.75 meter below the seafloor), and mono- and diglycosidic-iso-BDGTs (1G-, 2G-iso-BDGTs) detected in WORE sediments (0-20 cm).

Fig. 4. A composite chromatogram (A) showing methoxy-iso-GDGTs, iso-PDGTs, iso-BDGTs, iso-GDGTs, and methylated-iso-GDGTs (homo-caldarchaeol), and a schematic density map (B) of all determined tetraethers by LC-APCI-MS^2 analysis of TLE extracted from Peru Margin

342 sediments (ODP Leg 201, 1229A-12H3, 102.75 meter below the seafloor). The insert shows a
343 representative MS^2 spectrum of an ib-PDGT (*m/z* 1232.2; C_{81}).
344

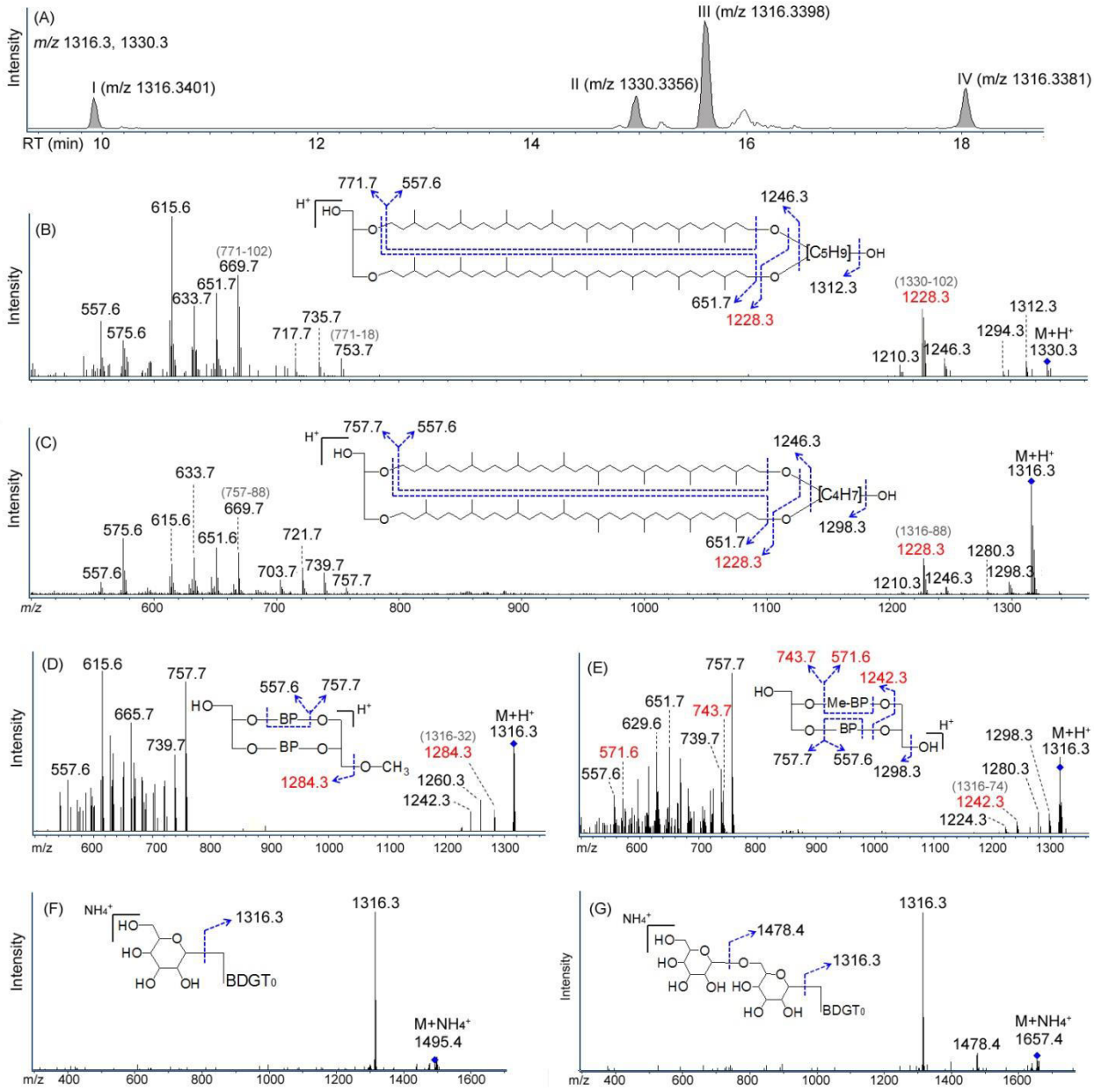
(A)
m/z 1316.3, 1330.3
I (m/z 1316.3401)
II (m/z 1330.3356)
III (m/z 1316.3398)
IV (m/z 1316.3381)
RT (min)
(B)
(C)
(D)
(E)
(F)
(G)
Intensity
m/z
M+H+
M+NH4+
BDGT0

Fig. 1.

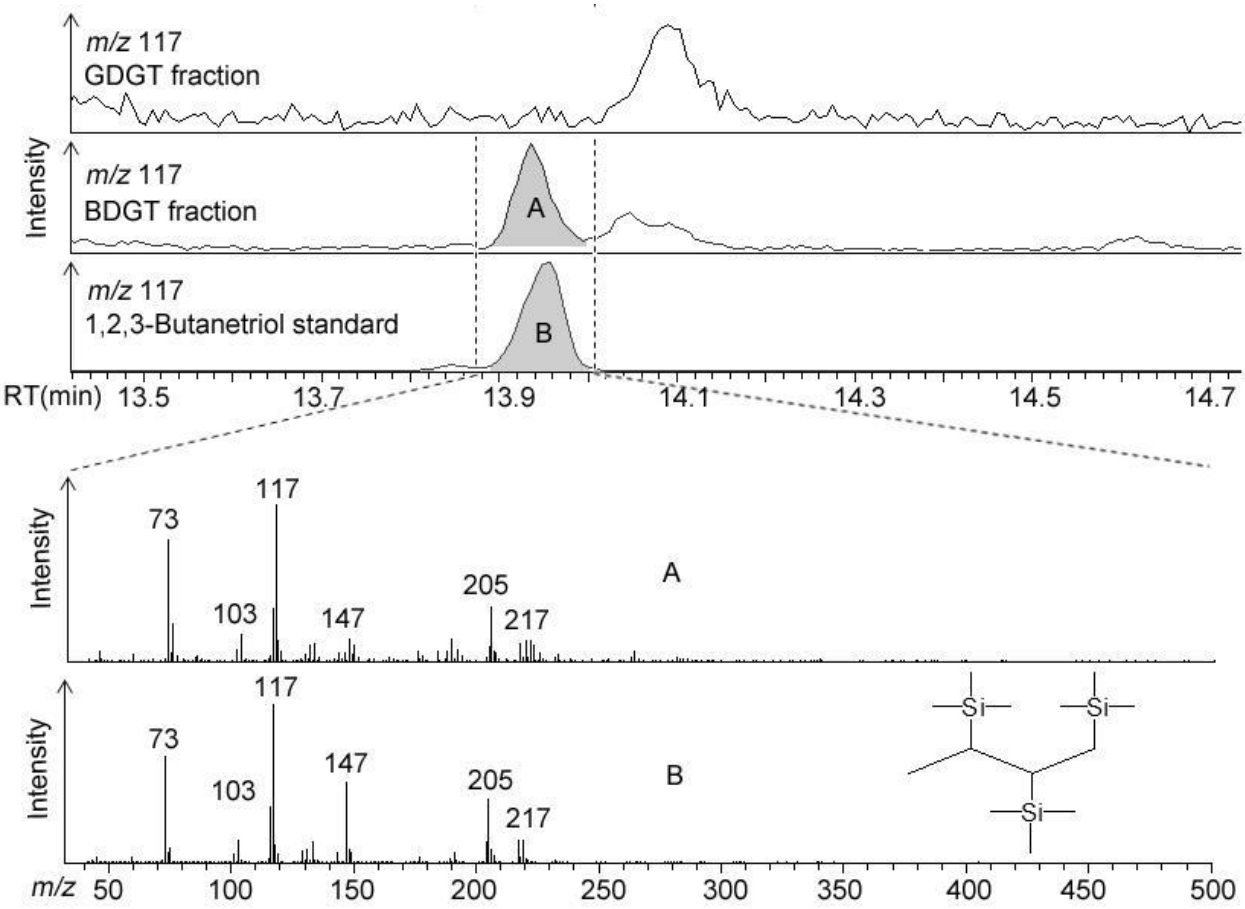
m/z 117
GDGT fraction
Intensity
m/z 117
BDGT fraction
A
m/z 117
1,2,3-Butanetriol standard
B
RT(min) 13.5 13.7 13.9 14.1 14.3 14.5 14.7
Intensity
73
117
103
147
205
217
A
Intensity
73
117
103
147
205
217
B
Si
Si
Si
m/z 50 100 150 200 250 300 350 400 450 500

Fig. 2.

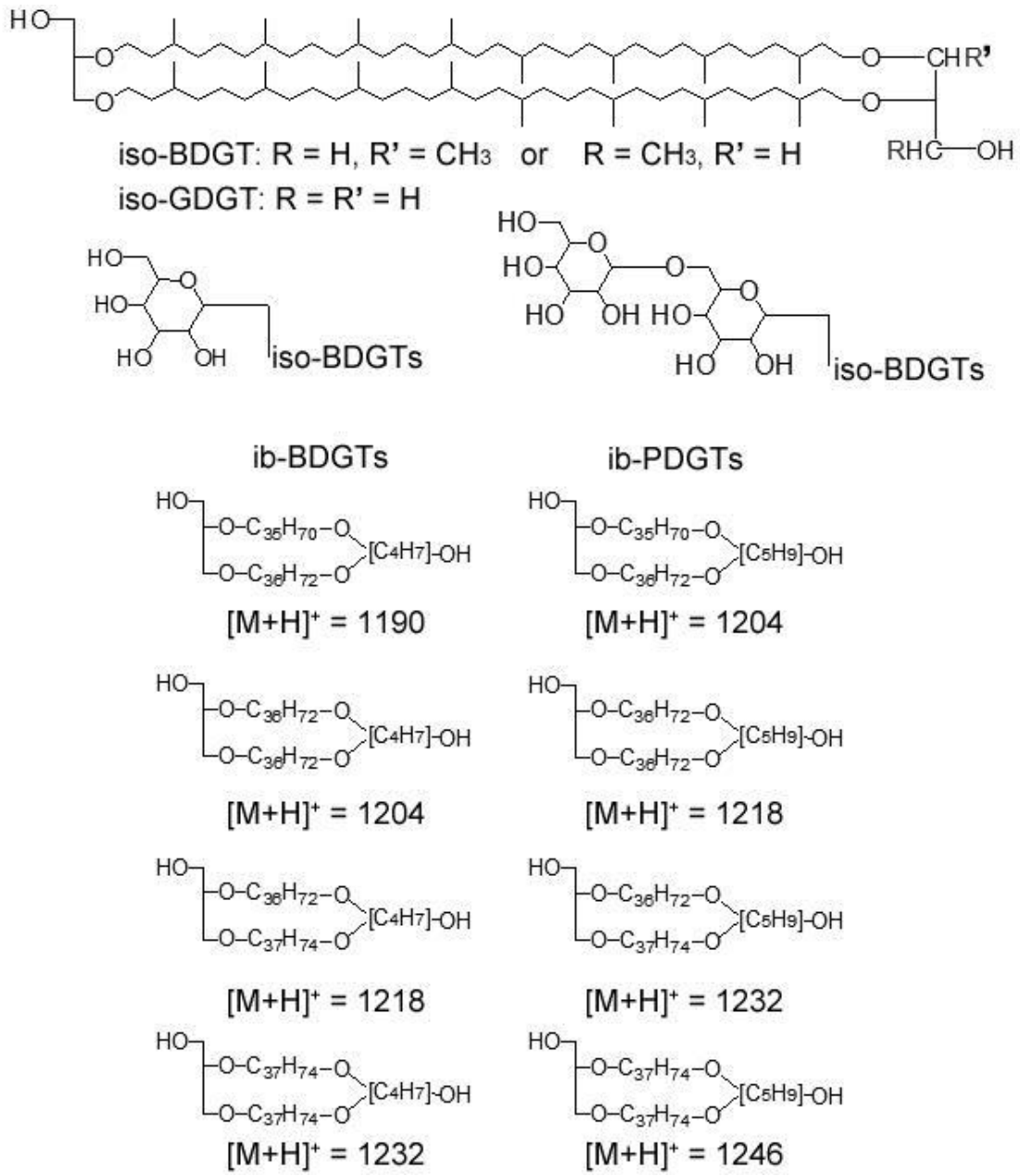
iso-BDGT: R = H, R' = CH3 or R = CH3, R' = H
iso-GDGT: R = R' = H
iso-BDGTs
iso-BDGTs
ib-BDGTs
ib-PDGTs
[M+H]+ = 1190
[M+H]+ = 1204
[M+H]+ = 1204
[M+H]+ = 1218
[M+H]+ = 1218
[M+H]+ = 1232
[M+H]+ = 1232
[M+H]+ = 1246

Fig. 3.

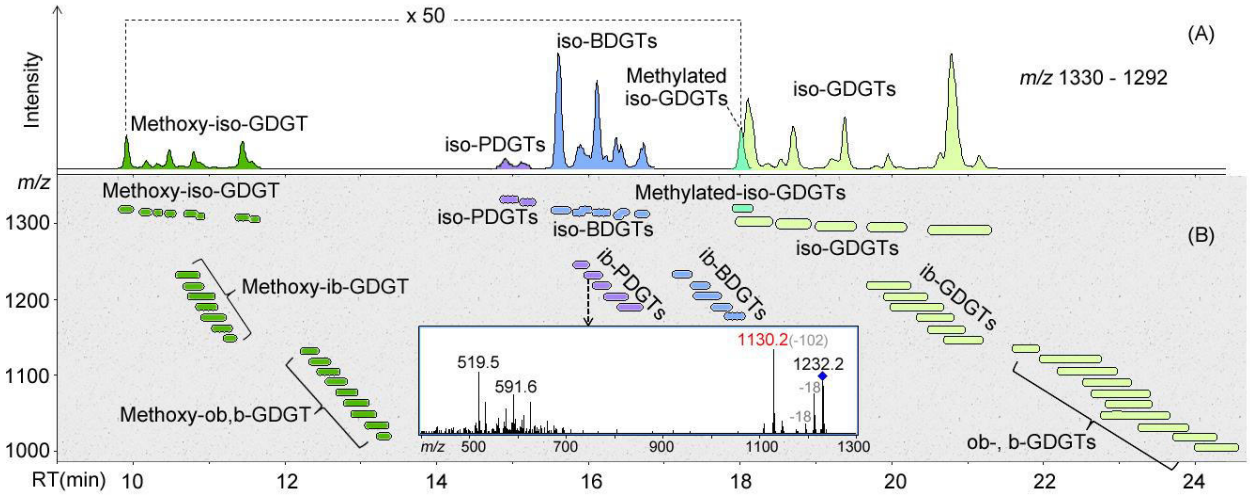
x 50
Intensity
(A)
iso-BDGTs
Methylated
iso-GDGTs
iso-GDGTs
m/z 1330 - 1292
Methoxy-iso-GDGT
iso-PDGTs
m/z
Methoxy-iso-GDGT
iso-PDGTs
iso-BDGTs
Methylated-iso-GDGTs
iso-GDGTs
(B)
ib-PDGTs
ib-BDGTs
ib-GDGTs
Methoxy-ib-GDGT
1130.2(-102)
519.5
591.6
1232.2
-18
-18
m/z 500 700 900 1100 1300
Methoxy-ob,b-GDGT
ob-, b-GDGTs
1300
1200
1100
1000
RT(min) 10 12 14 16 18 20 22 24

Fig. 4.